International Journal of Heat and Mass Transfer 52 (2009) 1464–1471

Contents lists available at ScienceDirect

International Journal of Heat and Mass Transfer

journal homepage: www.elsevier.com/locate/ijhmt

A node-based smoothed point interpolation method (NS-PIM) for thermoelastic problems with solution bounds

S.C. Wu [a,b,*], G.R. Liu [b,c], H.O. Zhang [a], G.Y. Zhang [c]

[a] State Key Laboratory of Digital Manufacturing and Equipment and Technology, School of Mechanical Science and Engineering, Huazhong University of Science and Technology, Wuhan 430074, PR China
[b] Centre for Advanced Computations in Engineering Science (ACES), Department of Mechanical Engineering, National University of Singapore, 9 Engineering Drive 1, Singapore 117576, Singapore
[c] Singapore-MIT Alliance (SMA), E4-04-10, 4 Engineering Drive 3, Singapore 117576, Singapore

ARTICLE INFO

Article history:
Received 18 January 2008
Received in revised form 29 June 2008
Available online 7 October 2008

Keywords:
Numerical method
Thermoelasticity
Solution bounds
Heat transfer
Gradient smoothing
Nodal integration

ABSTRACT

A node-based smoothed point interpolation method (NS-PIM) is formulated to analyze steady-state thermoelastic problems. In this approach, shape functions are constructed using the point interpolation method (PIM), which permits the straightforward enforcement of essential boundary conditions. The smoothed Galerkin weak form is then used to construct discretized system equations using smoothing domains constructed based on nodes. The bound property, accuracy and convergence of the present formulation are studied using 1D and 2D thermoelasticity problems. It is found that the computed temperature and its resulted gradient are in very good agreement with the *analytical* results or those obtained using the finite element method (FEM). Compared with the 3-node triangular FEM, the NS-PIM can achieve better accuracy and higher convergence in energy norm using the same linear triangular mesh. Together with the FEM, we now for the first time have a simple way to obtain both upper and lower bounds of the exact solution to thermoelasticity problems.

1. Introduction

The finite element method (FEM) has become one of the most widely used numerical techniques in solving various engineering problems. However, FEM has some inherent shortcomings due to its strong reliance on element meshes. To tackle these problems, meshfree methods have been recently developed with remarkable progress, such as the element-free Galerkin method (EFG) [1], the meshless local Petrov–Galerkin method (MLPG) [2], the reproducing kernel particle method (RKPM) [3], etc.

The meshfree point interpolation method (PIM) [4] is formulated normally using the Galerkin weak form, where the shape functions are constructed through simple interpolation based on a small set of nodes in a local support domain that can be overlapping. By using the nodal integration scheme [5], a node-based smoothed PIM (NS-PIM or LC-PIM termed in the original paper) has been proposed [6]. The NS-PIM can ensure at least linear consistency, the conformability of displacement, and the monotonic convergence of numerical results. Furthermore, the simple schemes for selecting local supporting nodes based on the background triangles make the NS-PIM very efficient. The NS-PIM has been formulated for 1D, 2D and 3D solid mechanics problems [6,7]. A theoretical study and an intensively numerical investigation on the NS-PIM have been conducted by Liu and Zhang [8]. Properties of the NS-PIM have been found and proven, including the very important upper bound property, meaning that the NS-PIM can provide upper bound solution in energy norm to the exact solution for elasticity problems with homogeneous essential boundary conditions.

In many manufacturing process especially containing rapid heating and solidification, metal parts or components will experience drastic changes in both temperature and its resulted gradient, which can usually result in extremely thermal strains and hence stress [9,10]. Experimental study on these kinds of systems can be expensive, time-consuming and difficult to acquire detailed thermal and mechanical behaviors. Computational means is therefore often preferred for studying these kinds of systems.

In this work, the NS-PIM is formulated for steady-state thermoelastic problems. The computational domain is firstly discretized into triangular cells. The shape functions [4] are then constructed using the polynomial PIM and local supporting nodes are selected based on the background triangles. Finally, discretized system equations are derived through the smoothed Galerkin weak form using node-based smoothing domains. 1D and 2D thermoelastic

* Corresponding author. Address: State Key Laboratory of Digital Manufacturing and Equipment and Technology, School of Mechanical Science and Engineering, Huazhong University of Science and Technology, Wuhan 430074, PR China. Tel.: +65 65164797.
E-mail address: wushengchuan@gmail.com (S.C. Wu).

0017-9310/$ - see front matter Crown Copyright © 2008 Published by Elsevier Ltd. All rights reserved.
doi:10.1016/j.ijheatmasstransfer.2008.09.001

Nomenclature

b	body force, N
h	convection coefficient, W/(m^2 · °C)
k	thermal conductivity, W/(m^2 · °C)
N	number of total field nodes
n	the unit outward normal component
Q_v	internal heat source, W/m^3
q_Γ	prescribed heat flux, W/m^2
t_Γ	given traction, N/m^2
T_a	known ambient temperature, °C
u_Γ	given displacement, m

Greek symbols

$\mathbf{\Phi}$	vector of PIM shape functions
σ, ε	stress and strain
$\bar{\varepsilon}, \bar{\varepsilon}^0$	smoothed and initial strain
δ	variational or delta operator
λ, μ, E, ν	Lamé's and elasticity constants
α	thermal expansion, 1/ °C
Ω	integration or problem domain
Γ	global or local boundary

Subscripts and superscripts

i, I, J	tensor or node indices
k	smoothing domain for node k
e	equivalent energy or error indicator
T, T	transpose symbol and error indicator

problems with mixed thermal boundary conditions are studied to examine the accuracy, convergence and most importantly the upper bound property of numerical solutions of the present NS-PIM.

2. Discretized system equations

Our numerical tests show that the NS-PIM works well for all kinds of meshes, including triangular types of meshes. We however prefer triangular mesh because it can be generated easily and even automatically for very complicated problem domains, leading to significant savings in manpower and hence the cost of the analysis project. Therefore, this work uses only 3-node triangular mesh shown in Fig. 1 as a background cells for node selection in creating the PIM shape functions and a base for creating node-based smoothing domains.

2.1. Gradient smoothing technique

For numerical integration, the problem domain Ω is partitioned into N smoothing domains Ω_k ($k = 1,2,\ldots,N$) with one for each node based on the background triangular mesh. The smoothing domain Ω_k for node k is created by connecting sequentially the mid-edge-points to the centroids of the surrounding triangles of node k.

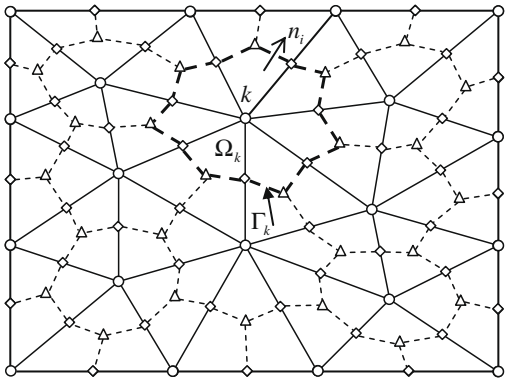

Fig. 1. Node-based polygonal smoothing domains are created based on triangular mesh, by sequentially connecting the mid-edge-points with centroids of surrounding triangles of node k. Ω_k is the smoothing domain of node k bounded by Γ_k and n_i is the unit outward normal to smoothing domains.

The node-based smoothing technique [5,11] is now applied to the *compatible* gradient of the primary field variable that can be displacement or temperature field for thermoelastic problems. The compatible gradient is obtained directly by differentiation to the PIM shape functions. The smoothing operation yields the following *smoothed* displacement gradient (strain) or temperature gradient:

$$\bar{\boldsymbol{\varepsilon}}_{IJ}(\mathbf{x}_k) = \frac{1}{A_k}\int_{\Omega_k} \boldsymbol{\varepsilon}_{IJ}(\mathbf{x}_k)\,\mathrm{d}\Omega \approx \frac{1}{2A_k}\int_{\Gamma_k} (u_I n_J + u_J n_I)\,\mathrm{d}\Gamma \tag{1}$$

where A_k is the area of smoothing domain, and u is the assumed displacement or temperature field. It should be noted that we use approximately equal in Eq. (1) to consider possible discontinuity in the assumed displacement and temperature fields [11] by the PIM shape functions. Only when the PIM shape functions are continuous, the approximately equal becomes equal.

Using the PIM approximation function $T(\mathbf{x}) = \mathbf{\Phi}^{\mathrm{T}}(\mathbf{x})\mathbf{q}$, the smoothed field gradient for interested node k can be expressed in the following matrix form in terms of nodal values of the field variable.

$$\bar{\boldsymbol{\varepsilon}}(\mathbf{x}_k) = \sum_{I\in D_k} \overline{\mathbf{B}}_{\mathbf{I}}^{\mathrm{T}}(\mathbf{x}_k)\mathbf{d}_{\mathbf{I}} \tag{2}$$

where D_k is the total number of nodes in the support domain of node k. For 2D thermoelasticity, the smoothed temperature gradient and strain can be expressed as

Smoothed temperature gradient : Smoothed strain :

$$\bar{\mathbf{g}}^{\mathrm{T}} = \{\nabla\bar{T}_1 \quad \nabla\bar{T}_2\} \qquad \bar{\boldsymbol{\varepsilon}}^{\mathrm{T}} = \{\bar{\varepsilon}_{11} \quad \bar{\varepsilon}_{22} \quad \bar{\varepsilon}_{12}\} \tag{3}$$

$$\overline{\mathbf{B}}_I^{\mathrm{T}}(\mathbf{x}_k) = [\bar{b}_{I1} \quad \bar{b}_{I2}] \qquad \overline{\mathbf{B}}_I^{\mathrm{T}}(\mathbf{x}_k) = \begin{bmatrix} \bar{b}_{I1} & 0 & \bar{b}_{I2} \\ 0 & \bar{b}_{I2} & \bar{b}_{I1} \end{bmatrix} \tag{4}$$

$$\bar{b}_{Ip} = \frac{1}{A_k}\int_{\Gamma_k} \varphi_I(\mathbf{x}) n_p(\mathbf{x})\,\mathrm{d}\Gamma \quad (p = 1,2) \tag{5}$$

where $\varphi(\mathbf{x})$ is the PIM shape functions [4] for field node I.

Using Gauss integration scheme along each segment of boundary Γ_k of the smoothing domain Ω_k, Eq. (5) can be rewritten in the following summation form as

$$\bar{b}_{Ip} = \frac{1}{A_k}\sum_{q=1}^{N_s}\left[\sum_{r=1}^{N_g} w_r \varphi_I(\mathbf{x}_{qr}) n_p(\mathbf{x}_q)\right] \tag{6}$$

where N_s is the number of segments of the Γ_k, N_g is the number of Gauss points distributed in each segment, and w_r is the corresponding Gaussian weight.

2.2. Smoothed Galerkin weak form

For steady-state thermoelastic problems without considering thermal–mechanical coupling and inertia, the primary field variables are the temperature and displacement. Considering first the temperature field in 2D anisotropic solid Ω bounded by Γ. The governing equation and boundary conditions are [12]:

$$(k_{ij}T_{,j})_{,i} + Q_v = 0 \quad \text{in } \Omega \quad \text{Problem domain studied} \tag{7}$$

$$T = T_\Gamma \quad \text{on } \Gamma_1 \quad \text{Essential boundary} \tag{8}$$

$$-n_i k_{ij} T_{,j} = q_\Gamma \quad \text{on } \Gamma_2 \quad \text{Heat flux boundary} \tag{9}$$

$$-n_i k_{ij} T_{,j} = h(T - T_a) \quad \text{on } \Gamma_3 \quad \text{Convection boundary} \tag{10}$$

$$-n_i k_{ij} T_{,j} = 0 \quad \text{on } \Gamma_4 \quad \text{Adiabatic boundary} \tag{11}$$

where k_{ij} is the thermal conductivity, Q_v is internal heat source, h is the convection coefficient, n_i is component of the unit outward normal to the boundary, q_Γ is the prescribed heat flux and T_a is the temperature of the surrounding medium.

After solving Eq. (7), the resulted thermal strain and stress can then be determined, by solving governing equations with displacement and stress boundary conditions [12]:

$$\sigma_{ij,j} + b_i = 0 \quad \text{in } \Omega \quad \text{Problem domain studied} \tag{12}$$

$$u_i = u_\Gamma \quad \text{on } \Gamma_u \quad \text{Displacement boundary} \tag{13}$$

$$\sigma_{ij} n_i = t_\Gamma \quad \text{on } \Gamma_t \quad \text{Stress boundary} \tag{14}$$

where u_Γ and t_Γ are the given displacement and traction, respectively, on the essential and natural boundaries, the heat and mechanics are linked by the following stress, strain and thermal expansion relation:

$$\sigma_{ij} = \delta_{ij}\lambda\varepsilon_{kk} + 2\mu\varepsilon_{ij} - \delta_{ij}(3\lambda + 2\mu)\alpha\Delta T \tag{15}$$

where λ and μ are Lamé's constants that can be derived from elastic constants (ν and E), α is the thermal expansion and ΔT is the change in temperature.

To obtain solutions of the thermoelastic system, temperature distribution inside the problem domain is found firstly. A weighted residual weak form of the partial differential Eq. (7) with four types of boundary conditions (8)–(11) over the entire domain can be written as a generalized functional I:

$$I(T) = \int_\Omega w[(k_{ij}T_{,j})_{,j} + Q_v]\,\mathrm{d}\Omega \tag{16}$$

where w denotes the sufficiently differentiable weight function of coordinate $\mathbf{x}^{\mathrm{T}} = [x_1, x_2]$. In this work, the PIM shape functions are selected also as the test function w, and thus the functional $I(T)$ can be written as:

$$I(T) = \int_\Omega \frac{1}{2}\left[k_{x_1}\left(\frac{\partial T}{\partial x_1}\right)^2 + k_{x_2}\left(\frac{\partial T}{\partial x_2}\right)^2\right]\mathrm{d}\Omega - \int_\Omega TQ_v\,\mathrm{d}\Omega + \int_{\Gamma_2} Tq_\Gamma\,\mathrm{d}\Gamma + \int_{\Gamma_3} hT\left(\frac{1}{2}T - T_a\right)\mathrm{d}\Gamma \tag{17}$$

With the temperature gradient presented in Eq. (17) replaced by smoothed gradient $\nabla\overline{T}$ in Eq. (3), the smoothed Galerkin weak form for heat transfer problems can be obtained as follows

$$\int_\Omega \delta(\nabla\overline{T})^{\mathrm{T}}\mathbf{k}\nabla\overline{T}\,\mathrm{d}\Omega - \int_\Omega \delta T^{\mathrm{T}}Q_v\,\mathrm{d}\Omega + \int_{\Gamma_2}\delta T^{\mathrm{T}}q_\Gamma\,\mathrm{d}\Gamma + \int_{\Gamma_3}\delta T^{\mathrm{T}}hT\,\mathrm{d}\Gamma - \int_{\Gamma_3}\delta T^{\mathrm{T}}hT_a\,\mathrm{d}\Gamma = 0 \tag{18}$$

Substituting the PIM approximation function [4] into Eq. (18), the discretized system equations can be finally expressed in the following matrix form:

$$[\overline{\mathbf{K}}^{\mathbf{T}} + \mathbf{K}^{\mathbf{M}}]\{\mathbf{q}\} = \{\mathbf{p}\} \tag{19}$$

where

$$\overline{\mathbf{K}}_{IJ}^{T} = \int_\Omega \overline{\mathbf{B}}_I^{\mathrm{T}}\mathbf{k}\overline{\mathbf{B}}_J\,\mathrm{d}\Omega = \sum_{L=1}^{N}\overline{\mathbf{B}}_I^{\mathrm{T}}(\mathbf{x}_L)\mathbf{k}\overline{\mathbf{B}}_J(\mathbf{x}_L)A_L \tag{20}$$

$$\mathbf{K}_{IJ}^{M} = \int_{\Gamma_3} h\boldsymbol{\Phi}_I^{\mathrm{T}}\boldsymbol{\Phi}_J\,\mathrm{d}\Gamma \tag{21}$$

$$\mathbf{p}_I = \int_\Omega \boldsymbol{\Phi}_I^{\mathrm{T}}Q_v\,\mathrm{d}\Omega - \int_{\Gamma_2}\boldsymbol{\Phi}_I^{\mathrm{T}}q_\Gamma\,\mathrm{d}\Gamma + \int_{\Gamma_3} hT_a\boldsymbol{\Phi}_I^{\mathrm{T}}\,\mathrm{d}\Gamma \tag{22}$$

$$\mathbf{k} = \begin{Bmatrix} k_{x_1} & 0 \\ 0 & k_{x_2} \end{Bmatrix} \tag{23}$$

where k_{x_1} and k_{x_2} are thermal conductivity in the x_1- and x_2-directions, respectively.

When the temperature field is obtained, the thermal stress and strain analysis can be sequentially performed using the smoothed Galerkin weak form [11]:

$$\int_\Omega \delta(\overline{\boldsymbol{\varepsilon}}(\mathbf{u}) - \overline{\boldsymbol{\varepsilon}}^0(\mathbf{u}))^{\mathrm{T}}\mathbf{D}(\overline{\boldsymbol{\varepsilon}}(\mathbf{u}) - \overline{\boldsymbol{\varepsilon}}^0(\mathbf{u}))\mathrm{d}\Omega - \int_{\Gamma_t}\delta\mathbf{u}^{\mathrm{T}}t_\Gamma\,\mathrm{d}\Gamma - \int_\Omega \delta\mathbf{u}^{\mathrm{T}}\mathbf{b}\mathrm{d}\Omega = 0 \tag{24}$$

in which $\overline{\boldsymbol{\varepsilon}}^0$ is the known smoothed initial strain obtained in the thermal analysis. In Eq. (24), the unknown smoothed strain field can be expressed in terms of the assumed displacement field for each node. The discretized linear system equations for the thermoelasticity problem can be obtained in the following matrix form:

$$\overline{\mathbf{K}}^{\mathbf{u}}\{\mathbf{d}\} = \{\overline{\mathbf{f}}\} \tag{25}$$

where

$$\overline{\mathbf{K}}_{IJ}^{u} = \int_\Omega \overline{\mathbf{B}}_I'^{\mathrm{T}}\mathbf{D}\overline{\mathbf{B}}_J'\,\mathrm{d}\Omega = \sum_{L=1}^{N}\overline{\mathbf{B}}_I'^{\mathrm{T}}(\mathbf{x}_L)\mathbf{D}\overline{\mathbf{B}}_J'(\mathbf{x}_L)A_L \tag{26}$$

$$\overline{\mathbf{f}}_I = \int_{\Gamma_t}\boldsymbol{\Phi}_I^{\mathrm{T}}t_\Gamma\,\mathrm{d}\Gamma + \int_\Omega \overline{\mathbf{B}}_I'\mathbf{D}\overline{\boldsymbol{\varepsilon}}_J^0\,\mathrm{d}\Omega + \int_\Omega \boldsymbol{\Phi}_I^{\mathrm{T}}\mathbf{b}\,\mathrm{d}\Omega \tag{27}$$

where $\mathbf{D}$ is the elastic constant matrix.

It can be easily seen from Eqs. (20) and (26) that the resultant linear system is symmetric and banded (due to the compact supports of PIM shape functions), which implies that the system equations can be solved efficiently. Excellent properties such as the convergence, softening effect and upper property of numerical solutions has been studied and can be found in [8,11].

3. Numerical examples

In this technical note, 1D and 2D problems are investigated using the NS-PIM with only linear PIM shape functions [6]. To examine quantitatively the performance of NS-PIM, the error indicators in temperature and energy norms are defined as

$$e_T = \sqrt{\frac{\sum_{i=1}^{N}(T_i^{\mathrm{exact}} - \overline{T}_i^{\mathrm{nume}})^2}{\sum_{i=1}^{N}(T_i^{\mathrm{exact}})^2}} \tag{28}$$

$$e_e = \frac{1}{A}\sqrt{\int_\Omega \frac{1}{2}[\boldsymbol{\varepsilon}^{\mathrm{exact}} - (\overline{\boldsymbol{\varepsilon}}^{\mathrm{nume}} - \overline{\boldsymbol{\varepsilon}}^0)]^{\mathrm{T}}\mathbf{D}[\boldsymbol{\varepsilon}^{\mathrm{exact}} - (\overline{\boldsymbol{\varepsilon}}^{\mathrm{nume}} - \overline{\boldsymbol{\varepsilon}}^0)]\,\mathrm{d}\Omega} \tag{29}$$

where A is the area of the problem domain. The superscript 'exact' denotes the exact or analytical solutions and 'nume' represents a numerical solution obtained using a numerical method including the present NS-PIM and FEM.

When the *exact* solution is not available, a *reference* solution computed from the FEM with a very fine mesh is then used instead. To study the bound property, the equivalent energy norm for heat transfer problem [13] is defined as follows

$$U_e = \int_\Omega \overline{\mathbf{g}}^{\mathbf{T}}\mathbf{k}\overline{\mathbf{g}}\,\mathrm{d}\Omega \tag{30}$$

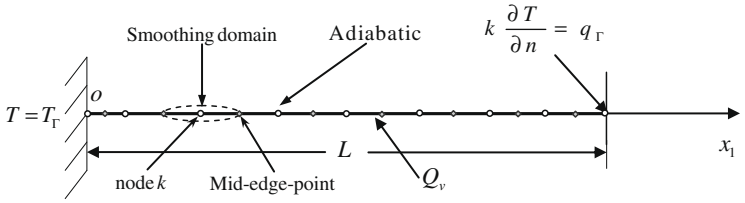

Fig. 2. Thermal fin problem (L = 1.0 m, T_Γ = 0 °C, q_Γ = 200 W/m^2 and Q_v = 100 W/m^3) discretized by a number of nodes. A typical smoothing domain (denoted by dashed curve) is constructed by connecting the midpoints of two neighboring line elements.

and the thermal strain energy can be calculated by the following formula

$$U_{eu} = \int_\Omega \frac{1}{2}(\bar{\boldsymbol{\varepsilon}} - \bar{\boldsymbol{\varepsilon}}^0)^{\mathrm{T}}\mathbf{D}(\bar{\boldsymbol{\varepsilon}} - \bar{\boldsymbol{\varepsilon}}^0)\,\mathrm{d}\Omega \tag{31}$$

3.1. 1D Thermal fin

The first example considered here is a 1D thermal fin with length L and uniform cross-sectional area subjected to a uniform inner heating, as shown in Fig. 2. The temperature T_Γ is given on the left end and heat flux q_Γ is specified on the right end.

Note that due to the delta property of PIM shape function, the boundary condition at the right-hand end can be imposed directly. In the computation, the related parameters are taken as L = 1.0 m, k = 5.0 W/(m · °C), q_Γ = 200 W/m^2, Q_v = 100 W/m^3 and T_Γ = 0 °C.

The *exact* temperature solution of this thermal fin can be easily found as

$$T(x_1) = -\frac{Q_v}{2k}x_1^2 + \frac{q_\Gamma + Q_v}{k}x_1 + T_\Gamma \tag{32}$$

The *exact* solution in equivalent energy can be calculated as below

$$U_e = \int_\Omega (\nabla\mathbf{T})^{\mathrm{T}}\mathbf{k}\nabla\mathbf{T}\,\mathrm{d}\Omega = 12666.6666\ (\mathrm{W}) \tag{33}$$

The convergence study is conducted using models with different numbers of uniformly distributed nodes, and the results in the equivalent energy are plotted in Fig. 3. It can be clearly seen that, as long as no less than 3 nodes are used in the model, the NS-PIM's solution in equivalent energy is always larger than that of the *exact* solution, while the FEM's solution is a lower bound of the exact solution.

Note that NS-PIM gives the same results as linear FEM when two nodes are used to discretize the problem domain. This is because only one element participants in the smoothing operation at each of these two nodes, and hence no smoothing effect takes place. Once more than two nodes are employed, the smoothing effect takes place for all the nodes in the interior of the problem domain, and the NS-PIM produces upper bound solutions as shown in Fig. 3. This important finding demonstrates the upper bound property of the NS-PIM for heat transfer problems, which is an important complement to the standard FEM.

3.2. 2D Thermoelasticity

To further examine the present NS-PIM, a 2D thermoelastic problem of a rectangle plate is then studied as shown in Fig. 4. The parameters used in the computation are taken as L = 0.05 m, H = 0.01 m, h = 1500 W/m^2 °C, T_a = 200 °C, T_Γ = 0 °C, k_1 = 15 W/(m · °C), k_2 = 10 W/(m · °C), q_Γ = −4000 W/m^2, α = 1.02 × 10^{-5}/°C, ν = 0.3, and E = 2.225 × 10^{11} Pa.

As no *exact* solution is available, a *reference* solution is obtained using ABAQUS© with very fine mesh of 329217 nodes for comparison purposes.

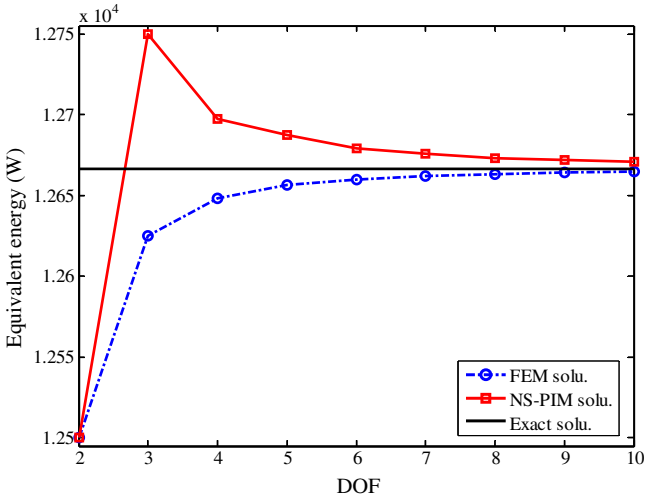

Fig. 3. Upper and lower bound solutions in equivalent energy for the 1D thermal fin problem obtained using the present NS-PIM and linear FEM, respectively.

3.2.1. Temperature and its gradients

Fig. 5 presents temperature distributions along the bottom edge of the rectangular plate obtained using linear NS-PIM and linear FEM, together with the *reference* solution. It can be found that the present NS-PIM solutions are in a very good agreement with the *reference* solution. Fig. 6 plots the distributions of temperature gradients in the x_2-direction of the problem domain computed using the present NS-PIM and FEM. It can be clearly seen that the distribution of the temperature gradient computed by the NS-PIM agrees well with the *reference* solution, and is more accurate than the FEM solution using the same triangular mesh.

Note that NS-PIM formulation here is derived from the smoothed Galerkin weak form, in which the gradient field is obtained using Eq. (3), and not the compatible in terms of usual displacement–strain relations. The NS-PIM mode satisfies better the equilibrium state of the system, and hence produces more accurate and smoother solution for the gradient. The same phenomenon has also been observed in the analysis of solid mechanic [6,8].

3.2.2. Thermal stress

Fig. 7 plots the numerical solutions of the x_1-component of the thermal stress. It can be seen that the computed stresses from the linear NS-PIM are more accurate and smoother than those from the linear FEM.

3.2.3. Bound property of solutions

It is well-known that the compatible FEM always obtains a lower bound of the exact solution in energy norm to elasticity problems. It is, however, much more difficult to bound the solution

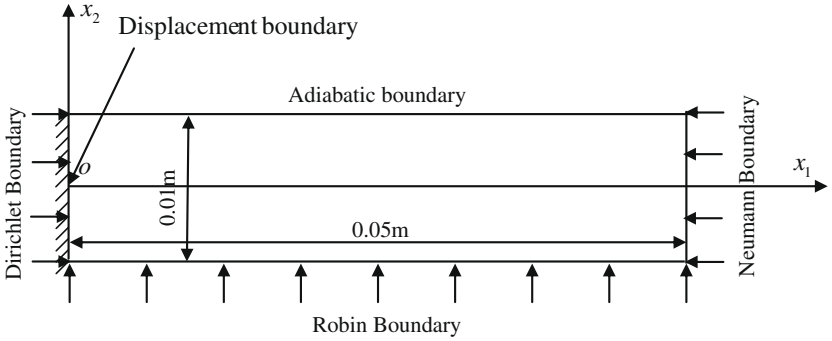

Fig. 4. Schematics of two-dimensional thermoelastic problem with the displacement, Dirichlet, Neumann and Robin boundary conditions.

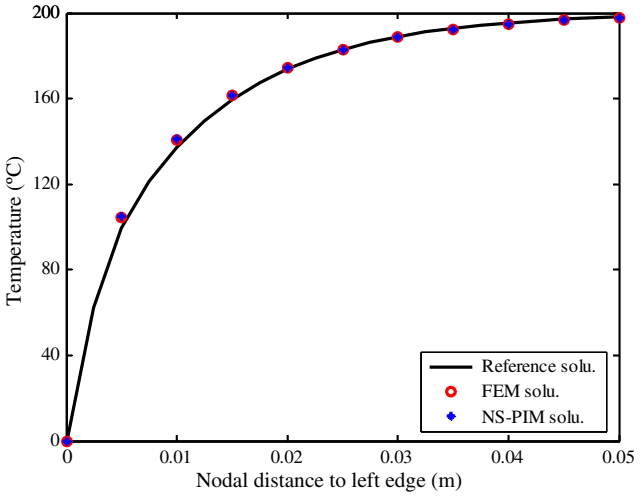

Fig. 5. Temperature distribution along the bottom edge of the rectangular plate.

from above for heat transfer and thermoelasticity problems. To examine the bound property of the NS-PIM, four models with regularly distributed 33, 105, 369 and 1377 nodes are created.

Fig. 8 shows the solutions in equivalent energy using the NS-PIM, FEM, together with the *reference* solution. It can be observed that the present NS-PIM provides an upper bound solution in equivalent energy norm for this 2D heat transfer problem with homogeneous essential boundary conditions ($T_\Gamma = 0$), and the compatible FEM model always gives a lower bound solution. This figure also shows that with the increase of DOFs, the solution of equivalent energy of the FEM model and the present NS-PIM model converges to the *reference* solution from below and above, respectively.

For thermoelastic analysis, we need to compute the stresses from the "imposed" thermal strains. In this case, the bound properties of NS-PIM and FEM can change. As shown in Fig. 9, thermal strain energy of the FEM model is larger than the *reference* one and converges from above with the increase in DOFs. On the contrary, thermal strain energy of the NS-PIM model is now smaller than the *reference* one and converges from below. This is because, the im-

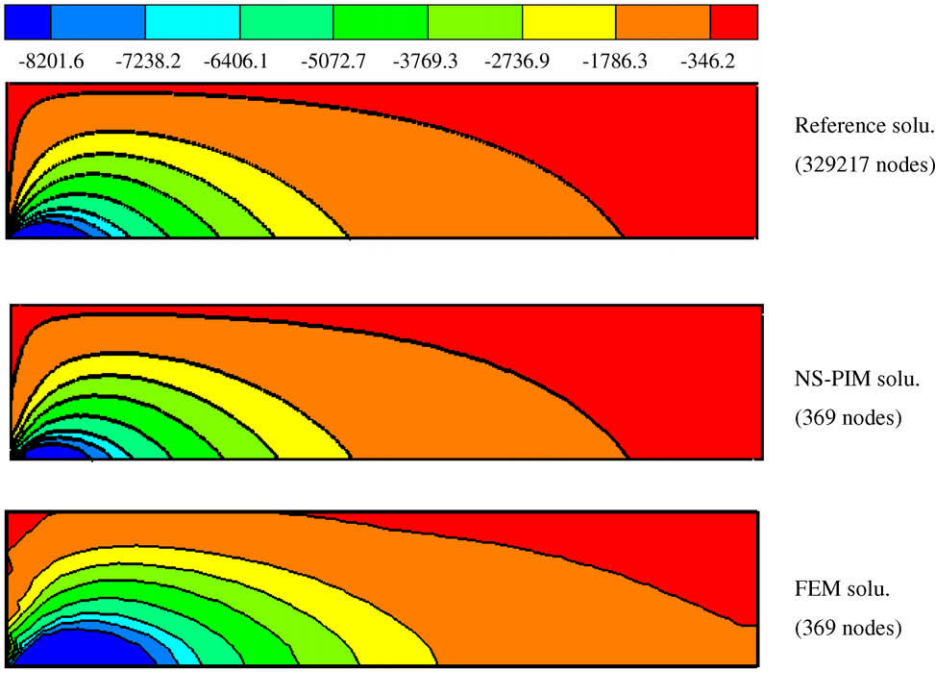

Fig. 6. Temperature gradient in the x_2-direction (°C/m).

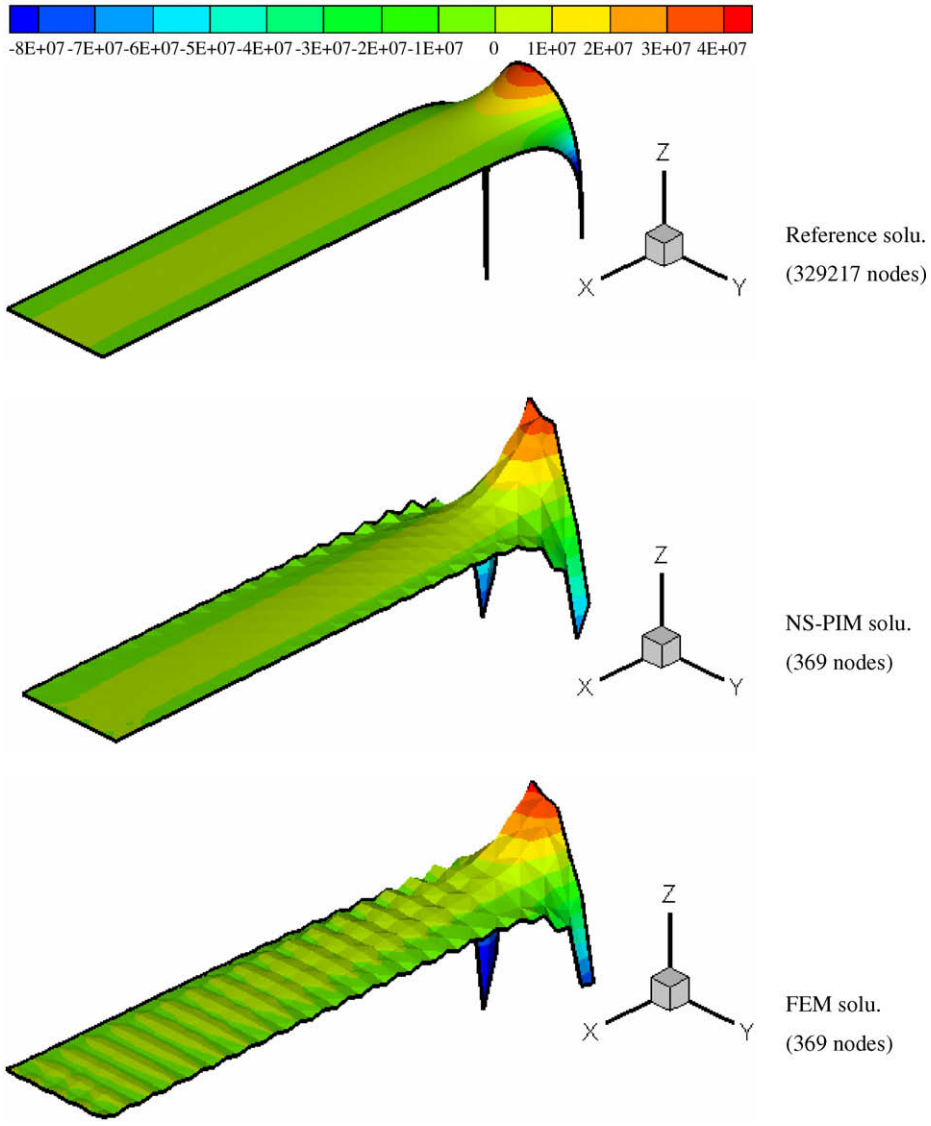

Fig. 7. Thermal stress fields in the x_1-direction (Pa).

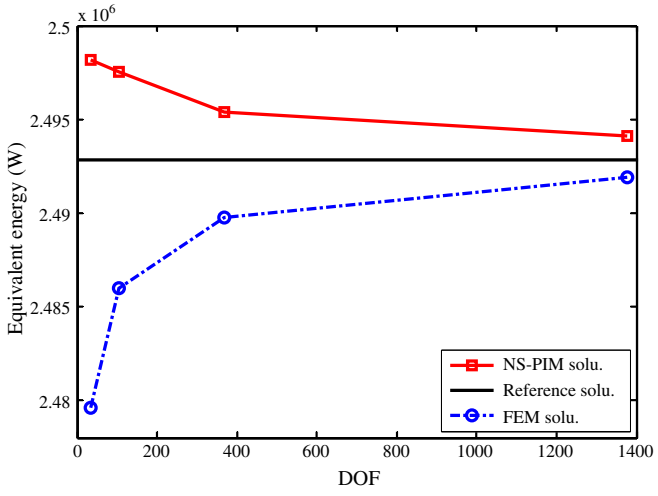

Fig. 8. Upper bound solution for equivalent energy obtained using the NS-PIM in heat transfer problems. The lower bound solution is obtained using linear FEM.

posed thermal strain acts as a kind of constraints, which makes the problem behaving like those with inhomogeneous displacement boundary conditions, resulting in the role exchange between the NS-PIM and FEM models in providing bounds. However, we can still bound the solutions from both sides.

3.2.4. Accuracy and convergence

This section further examines the accuracy and convergence of the present NS-PIM using the four models created in Section 3.2.3. Figs. 10 and 11 show the convergence curves in terms of temperature and thermal strain energy errors obtained using the linear NS-PIM and linear FEM against the average nodal spacing h, respectively. The convergence rate, R, is computed via linear regression upon the numerical results.

As shown in Figs. 10 and 11, the NS-PIM achieves better accuracy and higher convergence rate in both temperature and thermal strain energy, compared with those obtained from linear FEM. The results of the NS-PIM exhibit some behavior of the superconvergence with $R = 1.25$ that is significantly higher that the theoretical value of 1.0, as shown in Fig. 11.

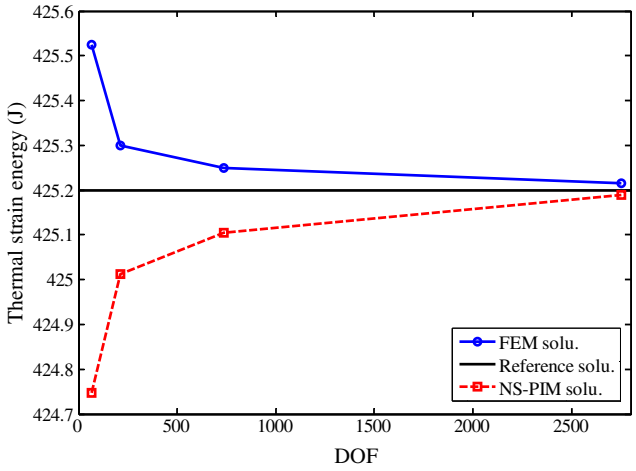

Fig. 9. Lower bound solution for thermal strain energy obtained using the NS-PIM in thermoelastic problems. The upper bound solution is obtained using linear FEM.

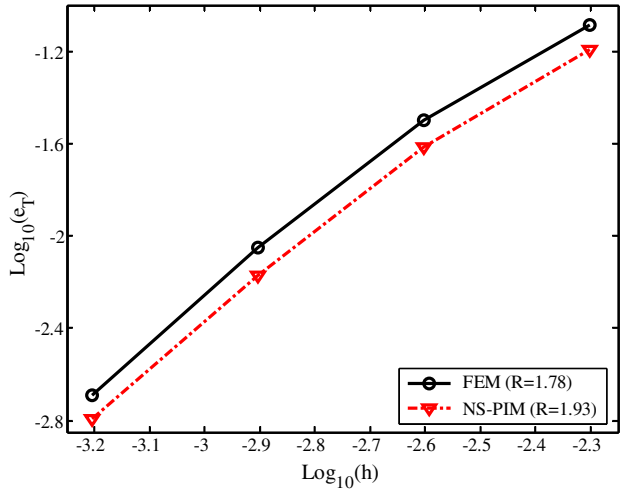

Fig. 10. Comparison of convergence rate in temperature norm obtained using the NS-PIM and linear FEM.

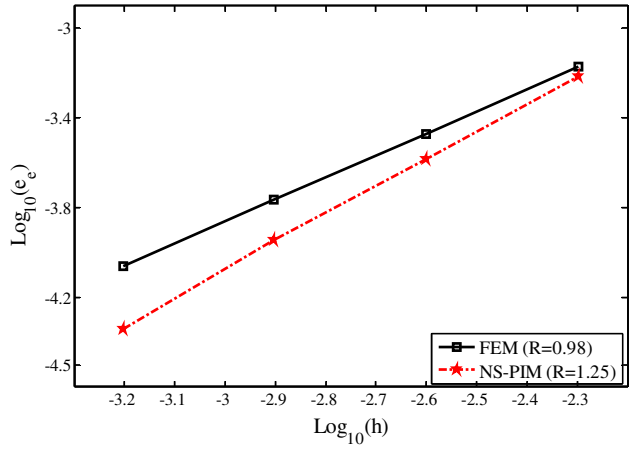

Fig. 11. Comparison of convergence rate of thermal strain energy norm obtained using the NS-PIM and linear FEM. Superconvergence behavior of the NS-PIM mode is observed.

4. Conclusions and discussions

The NS-PIM is further extended for thermoelastic problems in this work. Formulation based on the smoothed Galerkin weak form using node-based smoothing domains is first presented, and 1D and 2D example problems are then used to examine the accuracy, convergence and important solution bound properties. From this study, some remarks can be made as follows:

1. The NS-PIM works well with triangular mesh that can be easily generated thanks to the softening effects provided by the smoothing operation. This offers a very simple and effective way to overcome the usual "overly-stiff" behavior of the compatible FEM model.
2. For the problems studied in this paper, the linear NS-PIM can achieve higher accuracy and convergence in equivalent energy for thermal analysis, and in thermal strain energy in thermoelastic analysis, compared with the linear FEM.
3. Using both NS-PIM and FEM models of the same triangular mesh, we can now very conveniently bound the numerical solutions from both above and below for complicated thermoelastic problems, as long as the FEM model can be built.
4. The DOFs of NS-PIM and the FEM models are exactly the same when the same triangular mesh is used, and hence the computational cost for both NS-PIM and the FEM models are of the same order. When the same mesh is used, the CPU time for NS-PIM model is about the same as that of FEM model using the same mesh, if a full-matrix solver is used. Since the bandwidth of the NS-PIM model is about twice larger than the FEM counterpart, NS-PIM takes about twice more CPU time in solving the system equations when a bandwidth solved is used.

Note that the NS-PIM is not the only method that can produce an upper bound solution. There are other methods capable of providing upper bound solution for elasticity problems, such as force methods or equilibrium models based on the complementary energy principle [14].

Acknowledgements

The support of the National Natural Science Foundation of China under project No. 50474053, 50475134 and 50675081 is gratefully acknowledged. The authors also give sincerely thanks to the support of Centre for ACES and Singapore-MIT Alliance (SMA), National University of Singapore.

References

[1] T. Belytschko, Y.Y. Lu, L. Gu, Element-free Galerkin methods, Int. J. Numer. Meth. Eng. 37 (2) (1994) 229–256.
[2] S.N. Atluri, S.P. Shen, The Meshless Local Petrov–Galerkin (MLPG) Method, Tech Science Press, Balboa Blvd, USA, 2002.
[3] W.K. Liu, S. Jun, Y.F. Zhang, Reproducing kernel particle methods, Int. J. Numer. Meth. Eng. 20 (8–9) (1995) 1081–1106.
[4] G.R. Liu, Meshfree Methods: Moving Beyond the Finite Element Method, CRC Press, Boca Raton, USA, 2002.
[5] J.S. Chen, C.T. Wu, S. Yoon, Y.A. You, A stabilized conforming nodal integration for Galerkin meshfree methods, Int. J. Numer. Meth. Eng. 50 (2) (2001) 435–466.
[6] G.R. Liu, G.Y. Zhang, K.Y. Dai, Y.Y. Wang, Z.H. Zhong, G.Y. Li, X. Han, A linearly conforming point interpolation method (LC-PIM) for 2D solid mechanics problems, Int. J. Comput. Meth. 2 (4) (2005) 645–665.
[7] G.Y. Zhang, G.R. Liu, Y.Y. Wang, H.T. Huang, Z.H. Zhong, G.Y. Li, X. Han, A linearly conforming point interpolation method (LC-PIM) for three-dimensional elasticity problems, Int. J. Numer. Meth. Eng. 72 (13) (2007) 1524–1543.
[8] G.R. Liu, G.Y. Zhang, Upper bound solution to elasticity problems: a unique property of the linearly conforming point interpolation method (LC-PIM), Int. J. Numer. Meth. Eng. 74 (9) (2008) 1128–1161.
[9] M. Iwamoto, M. Ye, C.P. Grigoropoulos, R. Greif, Numerical analysis of pulsed laser heating for the deformation of metals, Numer. Heat Transfer A Appl. 34 (8) (1998) 791–804.

[10] S.C. Wu, H.O. Zhang, G.L. Wang, Numerical and experimental evaluation of the temperature and stress fields during plasma deposition dieless manufacturing, in: K.P. Rajurkar (Ed.), Proceedings of the 15th International Symposium on Electro-machining, Pittsburgh, USA, 2007, pp. 523–528.
[11] G.R. Liu, A generalized gradient smoothing technique and the smoothed bilinear form for Galerkin formulation of a wide class of computational methods, Int. J. Comput. Meth. 5 (2) (2008) 199–236.
[12] B.A. Boley, J.H. Weiner, Theory of Thermal Stress, John Wiley & Sons, New York, 1960.
[13] O.C. Zienkiewicz, R.L. Taylor, The Finite Element Method (V1: The Basis), fifth ed., Butterworth-Heinemann, Oxford, 2000.
[14] N. Pares, J. Bonet, A. Huerta, J. Peraire, The computation of bounds for linear functional outputs of weak solutions to the two-dimensional elasticity equations, Comput. Methods Appl. Mech. Eng. 195 (4–6) (2006) 406–429.